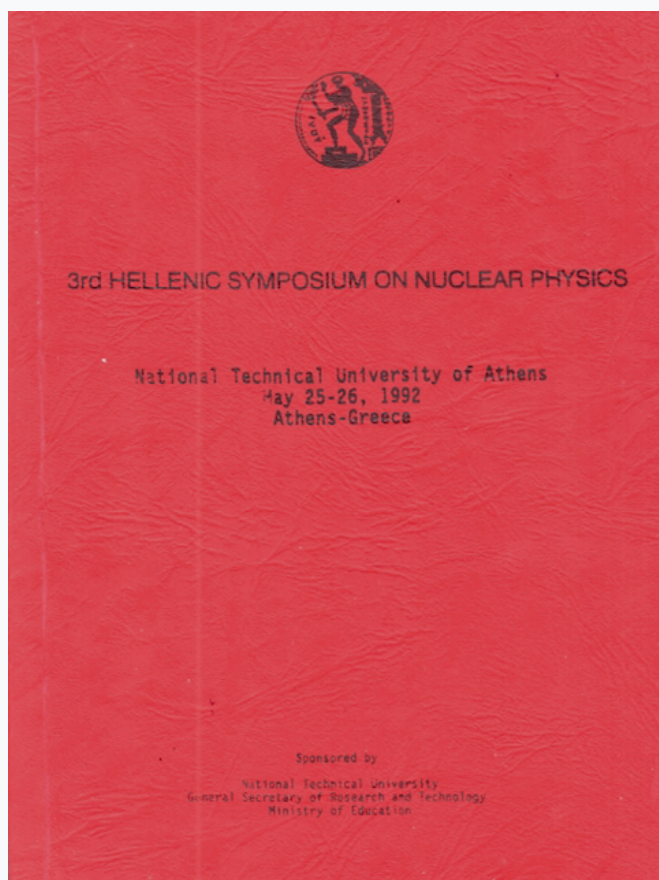


## HNPS Advances in Nuclear Physics

Vol 3 (1992)

HNPS1992



### High spin states of $^{195}\text{Hg}$

*N. Fotiades, S. Harissopulos, C. A. Kalfas, S. Kossionides, M. Serris, C. T. Papadopoulos, R. Vlastou, P. Fallon, S. M. Mullins, M. A. Riley, J. F. Sharpey-Schaffer*

doi: [10.12681/hnps.2380](https://doi.org/10.12681/hnps.2380)

### To cite this article:

Fotiades N., Harissopulos, S., Kalfas, C. A., Kossionides, S., Serris, M., Papadopoulos, C. T., Vlastou, R., Fallon, P., Mullins, S. M., Riley, M. A., & Sharpey-Schaffer, J. F. (2019). High spin states of  $^{195}\text{Hg}$ . *HNPS Advances in Nuclear Physics*, 3, 126–136. <https://doi.org/10.12681/hnps.2380>

## HIGH SPIN STATES IN $^{195}\text{Hg}$ \*

N.FOTIADES, S.HARISSOPULOS, C.A.KALFAS, S.KOSSIONIDES and M.SERRIS

NCSR Demokritos, Institute of Nuclear Physics

153 10 Agia Paraskevi, Athens, Greece

C.T.PAPADOPOULOS and R.VLASTOU

National Technical University of Athens,

157 73 Athens, Greece

P.FALLON, S.M.MULLINS, M.A.RILLEY, J.F.SHARPEY-SCHAFER

Oliver Lodge Laboratory, University of Liverpool,

Liverpool L69 3BX, U. K.

### Abstract

High spin states in  $^{195}\text{Hg}$ , populated using the  $^{150}\text{Nd}(^{48}\text{Ca}, 3n)$  reaction, were investigated by  $\gamma$ -ray spectroscopic techniques. Two backbendings are observed in the yrast band considered to be caused by the alignment of a pair of  $i_{13/2}$  and  $p_{3/2}$  neutrons respectively. The strong backbending behaviour observed in the negative parity side band is consistent with the alignment of a pair of  $i_{13/2}$  neutrons. The similarity with the corresponding backbendings in the neighbouring isotopes is impressive.

### 1. Introduction

The medium-mass Hg isotopes have been investigated during the last decade with growing interest because they are located between nuclei with large prolate deformation and spherical nuclei, in a transitional region which exhibits features of oblate deformation. In addition they reveal strong shape variations, depending on neutron number and spin, and effects of coexistence of various nuclear shapes.

---

\* Presented by N. Fotiades

The cranked shell model has been successfully applied to Hg isotopes. The calculations of routhians, aligned angular momenta and band crossing frequencies agree with the experimental results. Recently the superdeformation phenomenon came out in this region, before all in  $^{191}\text{Hg}$  and later in other isotopes of this region.

It was the purpose of this work to extend the rotational bands of  $^{195}\text{Hg}$ , evaluate the structure of the yrast region and establish the nature of band crossings. The experimental procedure and results of this investigation are described in this paper followed by a comparison with previous results for  $^{191}\text{Hg}$  and  $^{193}\text{Hg}$  and theoretical calculations for  $^{194}\text{Hg}$ .

## 2. Experimental Results

High spin states of  $^{195}\text{Hg}$  were investigated with the  $^{150}\text{Nd}(^{48}\text{Ca}, 3n)$  reaction. The  $^{48}\text{Ca}$  beam of 190 MeV was provided by the Tandem Accelerator at the SERC Daresbury Laboratory. Three stacked self-supporting foils of isotopically enriched  $^{150}\text{Nd}$ , each of  $530\mu\text{g}/\text{cm}^2$  thick, were used as target. For the in-beam spectroscopic measurements the TESSA-3 multidetector array of 16-Compton-suppressed germanium detectors was used. Event-by-event coincidence data were recorded and stored on magnetic tapes in order to be used for subsequent off-line analysis which enabled us to establish  $\gamma$ -ray cascades and hence the decay scheme. The events were gain matched, symmetrised and stored into a  $4096 \times 4096$  channel coincidence matrix. Fig.1.a shows the first quarter of this matrix, that is the part of Fig.1.b which is covered with cross lines. Source spectra of  $^{152}\text{Eu}$  were used in order to obtain the efficiency calibration for the summed spectra of the 16 detectors. Known transitions of  $^{195}\text{Hg}$  helped us to perform the energy calibration. By cutting slices on this matrix we were able to deduce the level scheme of  $^{195}\text{Hg}$ . A characteristic slice of the matrix is shown in Fig.1.c

The level scheme of  $^{195}\text{Hg}$  extracted from the analysis of all the slices of the matrix is shown in Fig.2. The excitation energy of the levels is given relative to the  $13/2^-$  state at 176.1 keV. The assignment of the observed rotational bands was made on the basis of previous measurements of the low lying states of  $^{195}\text{Hg}$  and by comparison with the

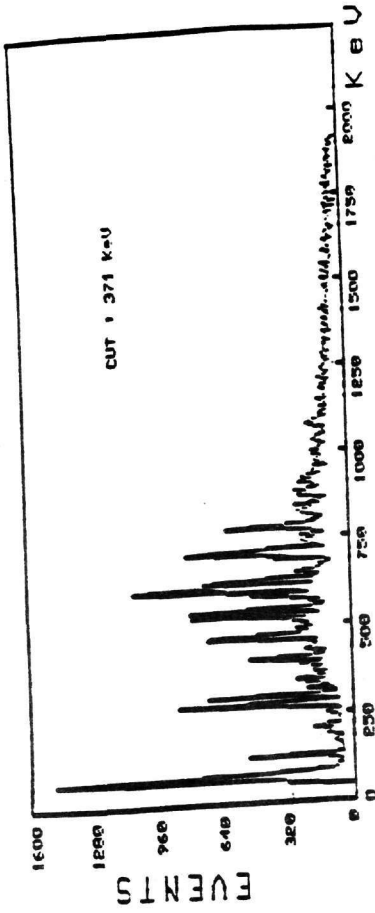
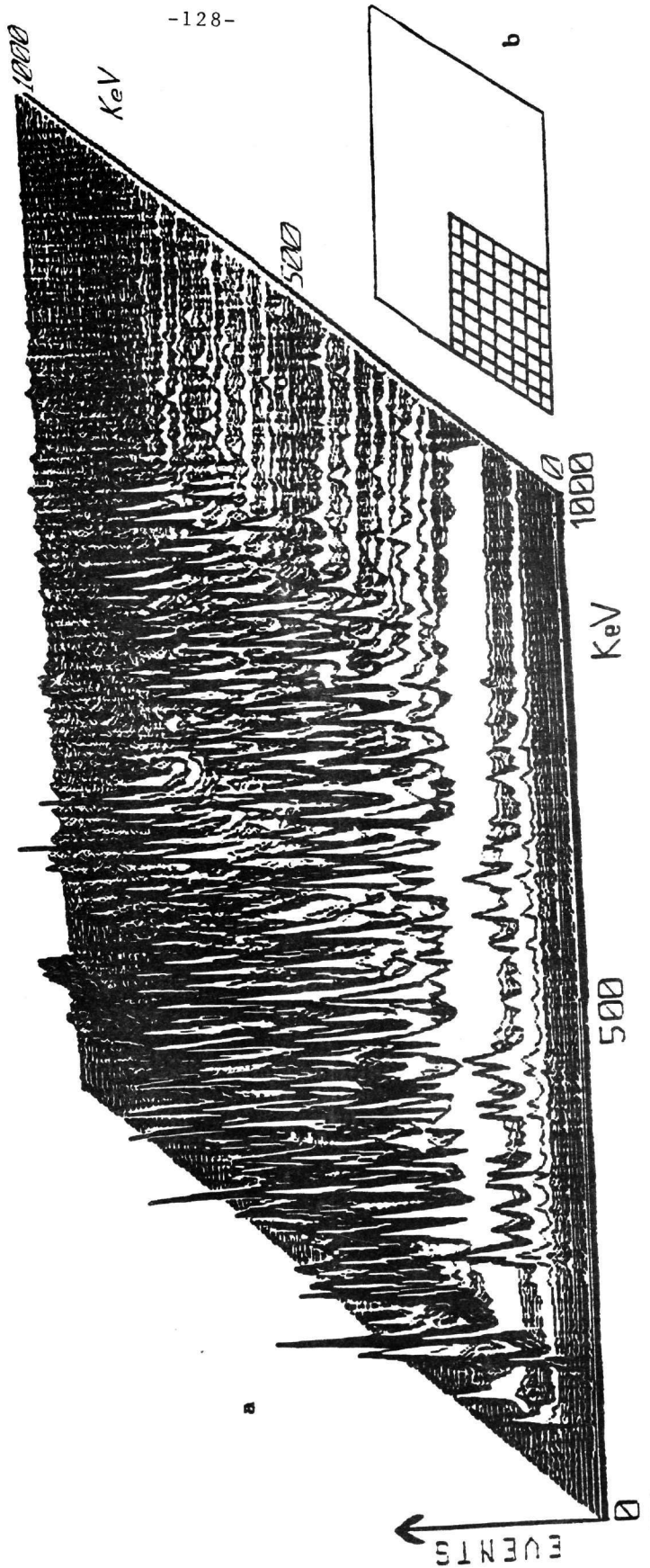


Fig. 1:  
a. First quarter of coincidence matrix  
b. Cross lines show the part of coincidence matrix in Fig. 1.a  
c. A characteristic slice on this matrix



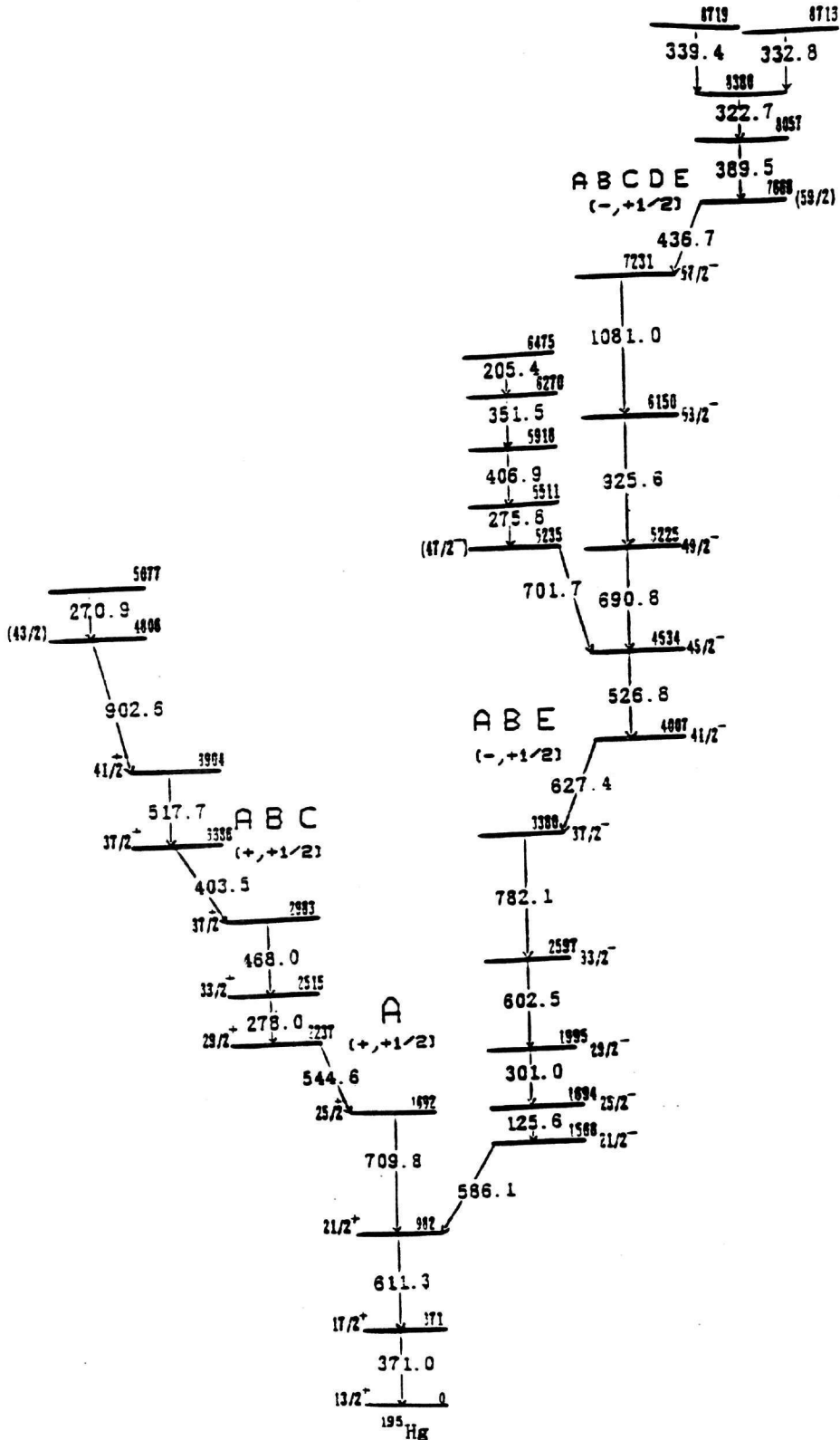


Fig. 2: Level scheme of  $^{195}\text{Hg}$ . Uncertainties of  $\gamma$ -rays between 0.2 and 0.5 keV depending on  $\gamma$ -ray intensity.

neighbouring isotopes<sup>1</sup>). This assignment is consistent with Nilsson levels for this mass region, where the neutron Fermi level is situated on the  $1/2^+ [660]i_{13/2}$ ,  $3/2^+ [651]i_{13/2}$  and  $1/2^- [521]p_{3/2}$  orbitals shown in Fig.3

In the level scheme the ABC band consists of only two transitions ( $E_\gamma(\text{keV}) = 278.468$ ). Three more energies, ( $E_\gamma(\text{keV}) = 710.8, 872.9, 1006.7$ ) belonging in the same band, were recently established in a paper by Mehta et al.<sup>2</sup>). The reaction used in this last work was  $^{198}\text{Pt}(a,7n)$  and led to a stronger population of the positive parity bands than the reaction reported in the present paper. The opposite is valid for the negative parity bands which seem to be populated more intensively in the present reaction. However, the additional three energies, which could not be seen clearly in our data, will be used for a better comparison with the neighbouring isotopes in section 3.

Experimental routhians and spin alignments have been extracted and they are presented in Fig.4 and Fig.5 respectively. As core of reference the Harris formula, with  $J_0 = 8\text{MeV}^{-1}\hbar^2$  and  $J_1 = 40\text{MeV}^{-3}\hbar^4$ , has been subtracted from the calculated experimental routhians. The values used in the above formula have been adopted from the literature<sup>1</sup>) for  $^{194}\text{Hg}$ ,  $^{193}\text{Hg}$ .

### 3. Discussion

#### a. Comparison with theory

A few years ago CSM calculations using a Nilsson potential have been performed for  $^{194}\text{Hg}$  by Hubel et al.<sup>1</sup>). From these calculations we can extract the following interesting features which we can tentatively apply to  $^{195}\text{Hg}$ :

i) The slopes of the neutron routhians A,B,C and D emanating from the  $i_{13/2}$  orbital are very steep, as it is apparent from Fig.6.a,b, giving rise to large alignments from the decoupling of these particles.

ii) The interaction energies of all band crossings are very small engendering strong backbending effects.

iii) The protons are expected to become important for band crossing effects at frequencies above 0.3MeV.

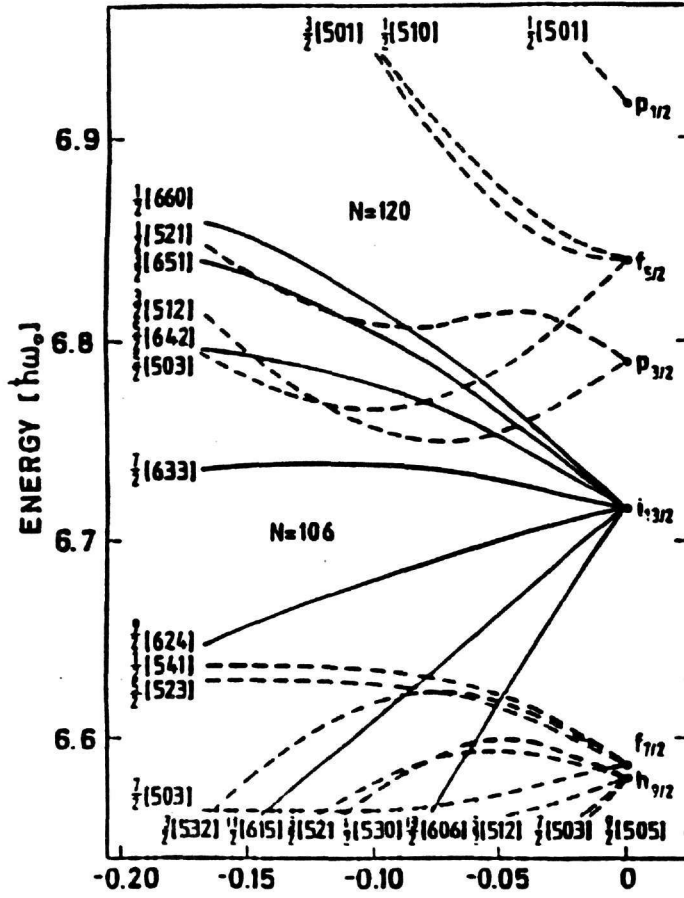


Fig. 3 Nilsson diagram for neutrons for the Hg nuclei (taken from ref.1)

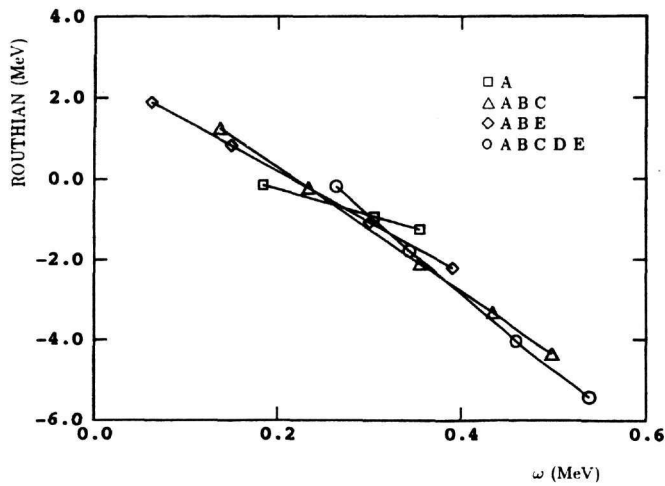


Fig. 4 Experimental routhians as a function of rotational frequency for  $^{195}\text{Hg}$

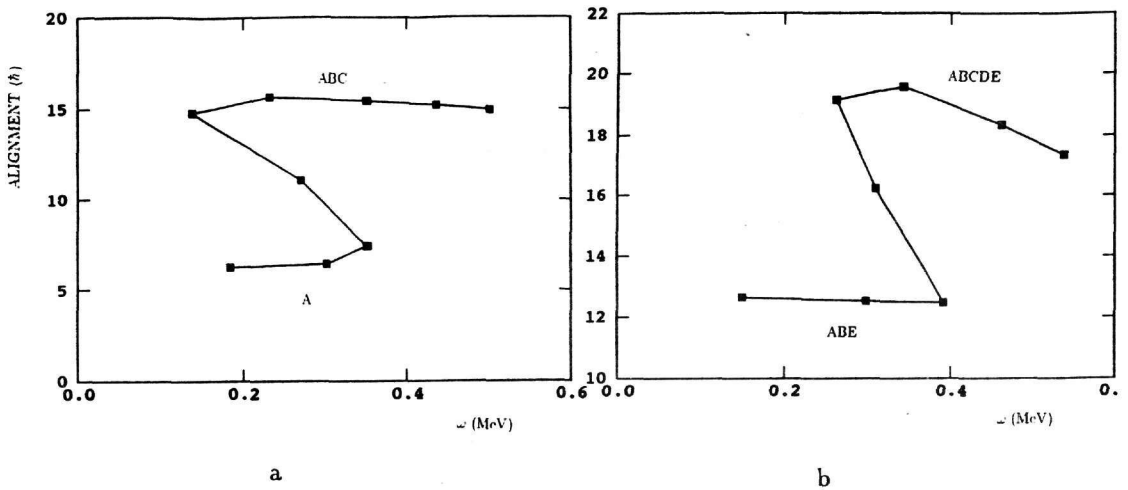


Fig. 5 Experimental alignments as a function of rotational frequency for  $^{195}\text{Hg}$

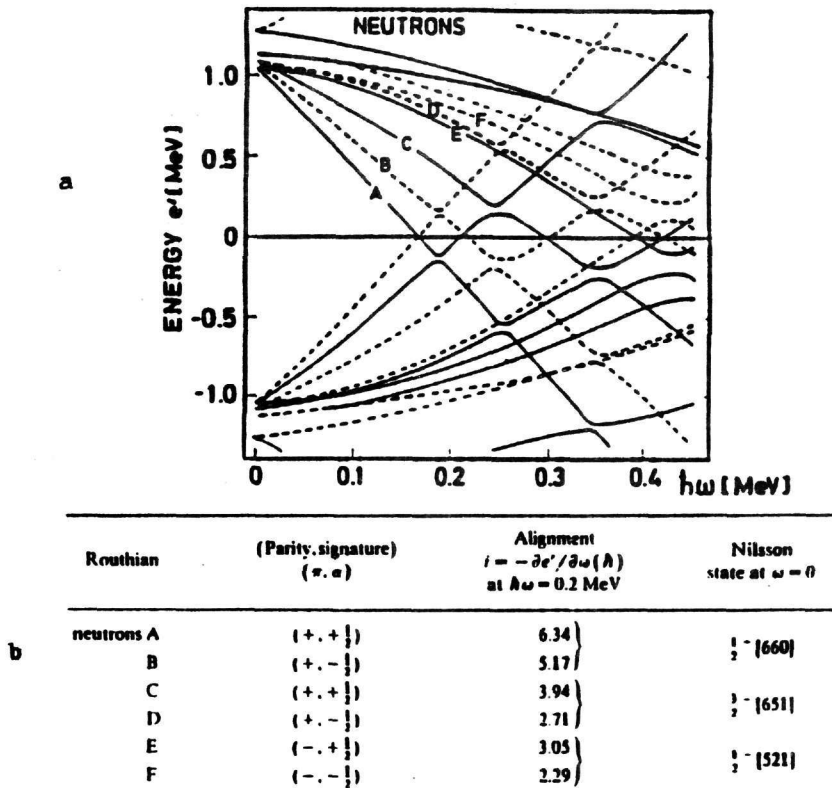


Fig. 6 a. Neutron routhians for  $^{194}\text{Hg}$

b. Properties of these routhians (taken from ref.1)

Indeed all these features are sustained by the conclusions drawn from the experimental data of  $^{195}\text{Hg}$ :

First and foremost, the experimental routhians shown in Fig.4 have steep slopes and produce large alignments (Fig.5).

The first backbending, observed in the alignment of the yrast band at 0.25MeV with a gain of alignment of  $9\hbar$  units (Fig.5.a), is consistent with a rotation alignment of a pair of  $i_{13/2}$  neutrons. Thus it is a BC crossing since the odd neutron blocks the AB crossing. The second backbending occurs in the negative parity band at 0.32MeV with  $6.8\hbar$  gain of alignment, as shown in Fig.5.b, and involves a neutron CD crossing. Both backbendings are strong and neutron-generated which is consistent not only with the theoretical predictions for  $^{194}\text{Hg}$  but also with the data of the neighbouring isotopes<sup>1</sup>).

Finally it should be mentioned that the experimentally observed band crossing frequencies are lower and the aligned angular momenta are higher than in other nuclei. The most probable reason for this is that medium mass Hg isotopes are expected to have small oblate deformation<sup>3</sup>) and hence small moment of inertia and so strong Coriolis forces acting on the  $i_{13/2}$  neutrons in the rotating cores break the pairs even at low rotational frequency.

#### b. Comparison with neighbouring isotopes

If one compares the level scheme of  $^{195}\text{Hg}$  with those of  $^{193}\text{Hg}$  and  $^{191}\text{Hg}$ <sup>1</sup>) will quickly note the similarities between these isotopes. In order to perform a detailed comparison of their behaviour it is convenient to transform the experimental quantities into the rotating frame and display them as a function of the rotational frequency. This was done according to the prescription given by Bengtsson and Frauendorf<sup>4</sup>).

Experimental routhians and spin alignments for  $^{191}\text{Hg}$ ,  $^{193}\text{Hg}$  and  $^{195}\text{Hg}$  are compared in Fig.7 and Fig.8 respectively. In Fig.7.d and Fig.8.b the ABCDE band of  $^{191}\text{Hg}$  is missing because this band has not been established yet. The similarity is more than striking. In all cases extremely sharp backbendings occur and large alignments can be observed (Fig.8). In addition the band crossing frequency is almost the same for the three isotopes. This effect does not appear in other nuclei, where, in some cases, differences from strong backbendings to gradual upbends can be observed between neighbouring isotopes. The most important

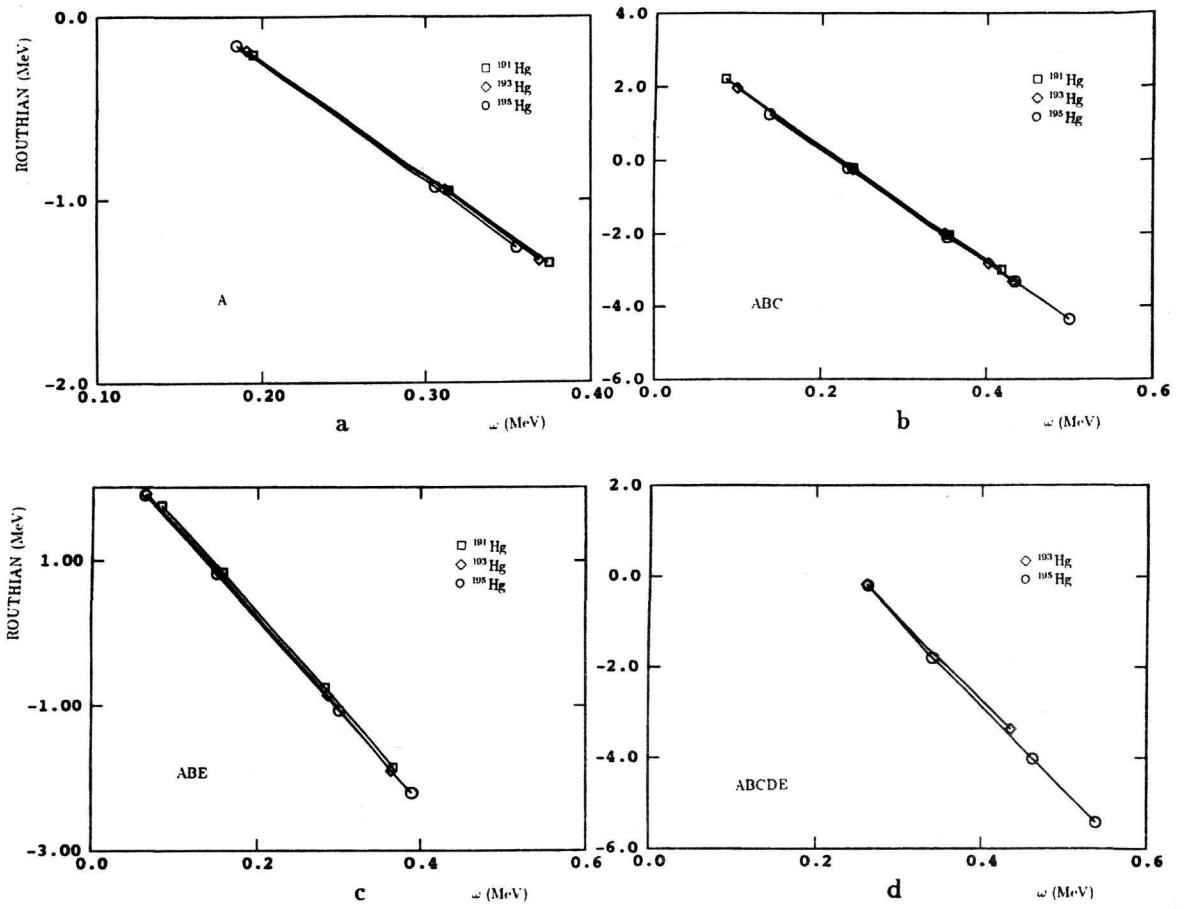


Fig. 7 Experimental routhians as a function of rotational frequency for  $^{191,193,195}\text{Hg}$

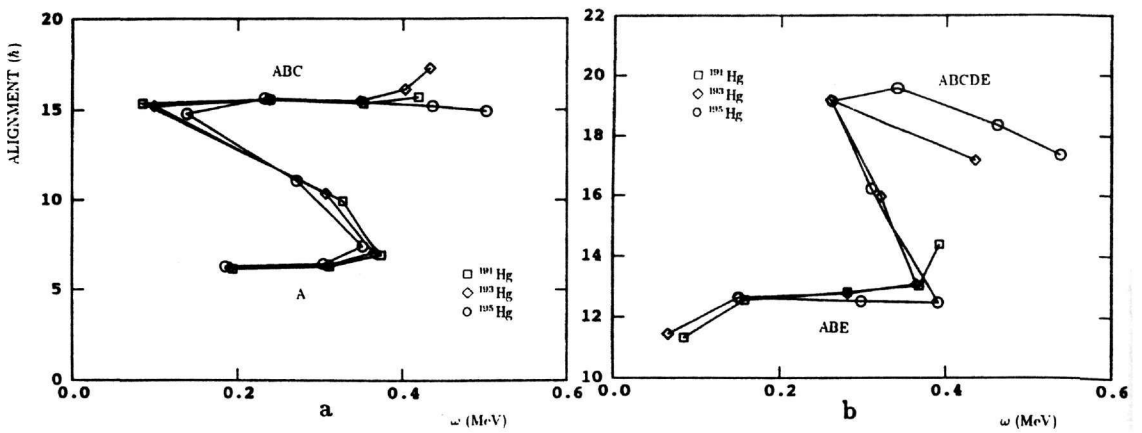


Fig. 8 Experimental alignments as a function of rotational frequency for  $^{191,193,195}\text{Hg}$

**Table 1** Summary of the most important features of the two bandbendings present in the negative parity bands of the 191, 193 and 195 isotopes of Hg, as they are calculated from the experimental data, together with theoretical results of calculations for <sup>194</sup>Hg taken from ref.1

Configuration	$(\pi, \alpha)$	Crossing		frequency (MeV)		Initial		alignment		$i(\hbar)$		Gain in alignment		$\Delta i(\hbar)$	
		<sup>191</sup> Hg	<sup>193</sup> Hg	exp	calc*	<sup>191</sup> Hg	<sup>193</sup> Hg	exp	calc*	calc*	calc*	exp	calc*	calc*	calc*
A $\rightarrow$ ABC	(+, +1/2)	0.26	0.26	0.26	0.25	6.4	6.4	6.4	6.4	6.3	6.3	9.3	9.2	9.0	9.1
ABE $\rightarrow$ ABCDE	(-, 1/2)	-	0.33	0.32	0.35	13.3	13.0	12.5	14.6	-	6.3	6.8	6.7		

\* calculations for <sup>194</sup>Hg ; values taken from ref.1

values for the comparison between theoretical and experimental behaviour are summarized in Table 1.

### c. Hints of a hidden phenomenon

In the level scheme of  $^{195}\text{Hg}$  five transition energies have been established above the ABCDE band, that is above 7231 keV level. Due to the low statistics of the experimental data the directional correlation ratios (DCO's) could not be established and hence the spins of the levels are uncertain. However similar transitions were established recently for  $^{191}\text{Hg}$  in a paper by Ye et al.<sup>5)</sup> suggesting a non-collective behaviour and a change of shape from oblate to prolate and for  $^{193}\text{Hg}$  in a paper by Roy et al.<sup>6)</sup> suggesting a collective behaviour appropriate for tilted axis cranking analysis. Keeping in mind the similarities in the behaviour of the Hg isotopes we can tentatively suggest that one of the two phenomena mentioned in the papers above is responsible for these transitions but it is impossible with the present data to conclude on which of them is hidden above 7231 keV level.

### References

- [1] H.Hubel, A.P.Byrne, S.Ogaza, A.E.Stuchbery and G.D.Dracoulis,  
Nucl.Phys. A453 (1986) 316
- [2] D.Mehta, Y.K.Agarwal, K.P.Blume, S.Heppner, H.Hubel, M.Murzel,  
K.Theine, W.Gast, G.Hebbinghaus, R.M.Lieder and W.Urban,  
Z. Phys. A339 (1991) 317-323
- [3] M.T.Esat, D.C.Kean, R.H.Spear, M.P.Fewell and A.M.Baxter,  
Phys.Lett. 72B (1977) 49
- [4] R.Bengtsson and S.Frauentorf, Nucl.Phys. A327 (1979) 139
- [5] D.Ye, R.V.F.Janssens, M.P.Carpenter, E.F.Moore, I.Ahmad, K.B.Beard,  
Ph.Benet, M.W.Drigert, U.Garg, Z.W.Grabowski, T.L.Khoo, F.L.H.Wolfs,  
T.Bengtsson and I.Ragnarsson,  
Phys.Lett. 236B (1990) 7
- [6] N.Roy, J.A.Becker, E.A.Henry, M.J.Brinkman, M.A.Stoyer, J.A.Cizewski,  
R.M.Diamond, M.A.Deleplanque, F.S.Stephens, C.W.Beausang, J.E.Draper,  
to be published.